

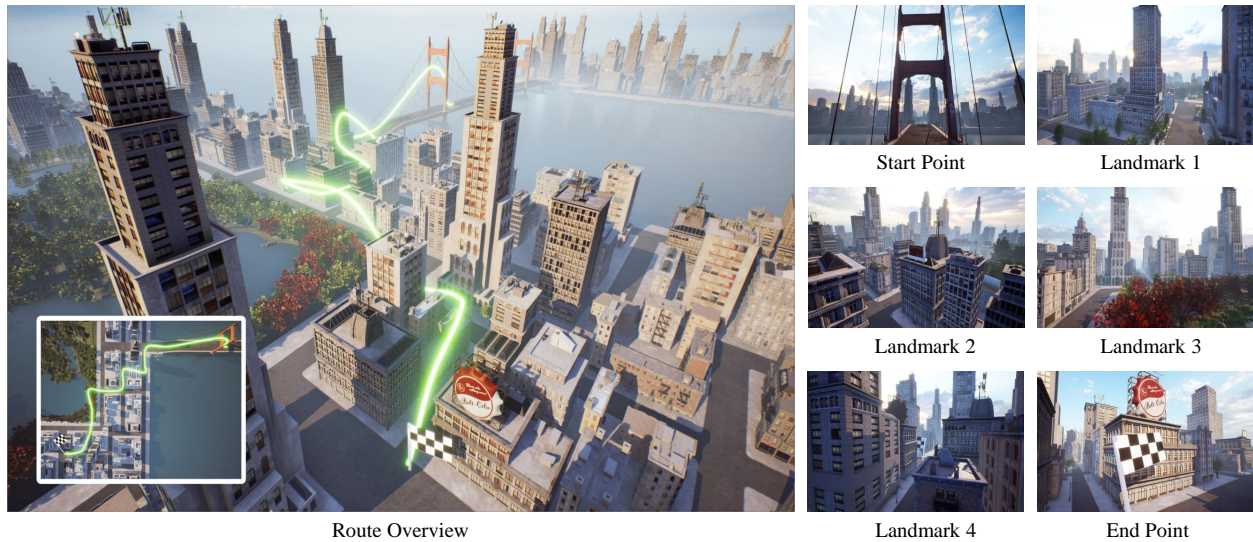
# AerialVLN : Vision-and-Language Navigation for UAVs

Shubo Liu<sup>1†</sup> Hongsheng Zhang<sup>1†</sup> Yuankai Qi<sup>2</sup> Peng Wang<sup>1\*</sup> Yanning Zhang<sup>1</sup>  
Qi Wu<sup>2</sup>

<sup>1</sup>Northwestern Polytechnical University

<sup>2</sup>University of Adelaide

{shubo.liu, hongsheng.zhang}@mail.nwpu.edu.cn, qykshr@gmail.com,  
{peng.wang, ynzhang}@nwpu.edu.cn, qi.wu01@adelaide.edu.au



**Instruction:** Take off, fly through the tower of cable bridge and down to the end of the road. Turn left, fly over the five-floor building with a yellow shop sign and down to the intersection on the left. Head to the park and turn right, fly along the edge of the park. March forward, at the intersection turn right, and finally land in front of the building with a red billboard on its rooftop.

Figure 1: An intelligent agent should be able to follow given natural language instructions and navigate to the destination in an unseen environment with visual perceptions along the way. The green line shows the agent’s ground truth trajectory, and the chequered flag represents the end of it.

## Abstract

Recently emerged Vision-and-Language Navigation (VLN) tasks have drawn significant attention in both computer vision and natural language processing communities. Existing VLN tasks are built for agents that navigate on the ground, either indoors or outdoors. However, many tasks require intelligent agents to carry out in the sky, such as UAV-based goods delivery, traffic/security

patrol, and scenery tour, to name a few. Navigating in the sky is more complicated than on the ground because agents need to consider the flying height and more complex spatial relationship reasoning. To fill this gap and facilitate research in this field, we propose a new task named AerialVLN, which is UAV-based and towards outdoor environments. We develop a 3D simulator rendered by near-realistic pictures of 25 city-level scenarios. Our simulator supports continuous navigation, environment extension and configuration. We also proposed an extended baseline model based on the widely-used cross-modal-alignment (CMA) naviga-

<sup>†</sup>These authors contribute equally to this work

\*Corresponding Author

tion methods. We find that there is still a significant gap between the baseline model and human performance, which suggests AerialVLN is a new challenging task. Dataset and code is available at <https://github.com/AirVLN/AirVLN>.

## 1. Introduction

Recently, a bunch of vision-and-language navigation tasks, such as R2R [2], RxR [20], REVERIE [28], Touch-Down [7], Alfred [33], iGibson [23, 32, 36], have drawn a large amount of attention from different research communities like computer vision, natural language processing and robotics. These tasks as well as their datasets have greatly boosted the research of assembling the capabilities of vision and language understanding, cross-modality matching, path planning and reasoning [6, 8, 15, 18, 27]. However, all these VLN tasks are designed for ground-based agents, which means agents can only navigate indoors or outdoors on the ground. This overlooks another important application scenario: activities in the sky, which are becoming increasingly popular with the development of unmanned aerial vehicles (UAVs), especially multirotor. We can now use UAVs to enjoy spectacular scenes without going out of houses and they can be potentially utilized for goods delivery, traffic surveillance, search/rescue and security patrol [10, 11, 12].

To release humans from manually operating UAVs and to fill the research gap in the field of navigation in the sky, we propose a city-level UAV-based vision-and-language navigation task, named AerialVLN, and a corresponding dataset. Navigating in the sky is significantly different from that on the ground in several aspects. **First**, AerialVLN has a larger action space. Compared to conventional ground VLN [2, 7, 19, 20, 28], AerialVLN requires intelligent agents to additionally take actions such as “rise up” and “pan down” into consideration. Moreover, multirotors can move left/right without turning its head. **Second**, the outdoor environments of AerialVLN are much bigger and more complex. AerialVLN covers a large variety of city-level scenes. An intelligent agent is required to distinguish referred buildings/objects by their spatial relationship from a bird-view as shown in Figure 1. Although the TouchDown [7] task is also devised for outdoor navigation, its environments are static, while ours are interactive and dynamic. For example, our agent can land on a building, and the weather and illumination conditions can dynamically change in the environment. **Third**, to mimic multirotor flying in real life, our AerialVLN has a much longer path than ground VLNs. On average, our AerialVLN involves a path length of 661.8

units\*. There are about 9.7 referred objects in one instruction on average, which is more than 2.6 times as many as in the R2R dataset [2]. **Fourth**, intelligent agents must learn to avoid getting stuck on objects in 3D space. This is more challenging than avoiding obstacles when navigating on the ground as in VLN-CE [19] because agents have to estimate the 3D shapes of obstacles and the distance to obstacles. All these new characters render AerialVLN a different and highly challenging task.

AerialVLN is implemented using Unreal Engine 4 [14] and Microsoft AirSim plugins [31], which enables continuous navigation and near-realistic rendering. In total, we have collected 25 different city-level environments, covering a variety of scenes such as downtown cities, factories, parks, and villages, including more than 870 different kinds of objects. Our AerialVLN dataset consists of 8,446 flying paths obtained by experienced human UAV pilots who hold the AOPA (Aircraft Owners and Pilots Association) certificate. We pair each path with 3 instructions annotated by AMT workers in the standard dataset setting. Notably, we also align each sub-path to its sub-instruction, which enables fine-grained cross-modality matching learning. On average, up to 83 words are in each instruction, involving a large vocabulary of 4,470 words. Finally, we evaluate five baselines, including two golden standard VLN models in VLN, Seq2Seq model and cross-modal matching (CMA) model, and our proposed model to serve as starting baselines on AerialVLN.

## 2. Related Work

In this section, we review two types of closely related work: UAV navigation and Ground-based VLN.

**UAV Navigation.** Unmanned Aerial Vehicle (UAV) navigation has brought increasing attention in the last few decades. Early UAV autonomous navigation requires solving the challenges of perceiving, mapping, localisation, decision-making (path-planning), action-decomposing and controlling. Inertial UAV navigation and GPS-based methods are commonly used together since the former might cause significant errors due to accumulation, and the latter is usually unable to localise the vehicle in high precision [22, 26]. However, navigation in GPS-denied and unknown environments (such as cities with collapsed buildings or complex electromagnetic scenarios) becomes the bottleneck of intelligent UAVs. Vision-based navigation is then believed to be the solution to autonomous navigation [9, 24, 34].

The most similar works to ours are [3, 4, 13, 25] that language instructions are also provided. In [3, 4, 25], a

\*One unit equals one meter in our simulated city environment.

Task	Routes	Instructions	Features	Language	Action Space	Path Len.	Actions	Vocab	Intr. Len.
R2R [2]	7,189	21,567	Indoor, discrete	Instruction	Graph-based	10.0	5	3.1k	29
RxR [21]	13,992	13,992	Indoor, discrete	Instruction	Graph-based	14.9	8	7.0k	129
CVDN [35]	7,415	2,050	Indoor, discrete	Dialog	Graph-based	25.0	7	4.4k	34
REVERIE [28]	7k	21,702	Indoor, discrete	Instruction	Graph-based	10.0	5	1.6k	18
SOON [37]	40K	3,848	Indoor, discrete	Instruction	Graph-based	16.8	9	1.6k	39
TouchDown[7]	9,326	9,326	Outdoor, discrete	Instruction	Graph-based	313.9	35	5.0k	90
VLN-CE [19]	4,475	13,425	Indoor, continuous	Instruction	2 DoF	11.1	56	4.3k	19
LANI [25]	6,000	6,000	Outdoor, continuous	Instruction	2 DoF	17.3	116	2.3k	57
ANDH [13]	6,269	6,269	Outdoor, continuous	Dialog	3 DoF	144.7	7	3.3k	89
AerialVLN	8,446	25,338	Outdoor, continuous	Instruction	4 DoF	661.8	204	4.5k	83
AerialVLN-S	3,916	11,748	Outdoor, continuous	Instruction	4 DoF	321.3	115	2.8k	82

Table 1: Comparison of existing vision-and-language navigation tasks. AerialVLN presents a city-level open environment dataset for aerial vision-and-language instruction-based navigation. Note that the en-US subset of RxR is considered for a fair comparison. Path length unit: meter.

quadcopter agent is required to navigate by following natural language instructions in only one closed virtual field. The environment is of size  $50 \times 50$  with  $6 \times 13$  landmarks. It has 6,000 instructions with an average length of 57 words and a vocabulary size 2,292. Agents are only allowed for horizontal movements (Forward, Left/Right and Stop). By contrast, our AerialVLN is much larger, more complex, and closer to real-world scenarios: AerialVLN provides 25k crowd-sourced natural language instruction with an average length of 83 words and a vocabulary size 4,470. AerialVLN has 870 different kinds of objects and allows agents to move in 4-DOF as multirotor (Forward, Turn Left/Right, Ascent/Descend, Move Left/Right and Stop). Moreover, AerialVLN presents 25 different open city-level environments, which enables intelligent agents to be trained and tested more comprehensively. Compared to ANDH [13], which focuses on dialogue-based aerial VLN with bird-view image input, our AerialVLN task requires agents to navigate with a first-person view and our environments are interactive and dynamic, which requires agents to learn to avoid obstacles. Regarding path length and data amount, our AerialVLN is four times of ANDH. More comparisons can be found in Table 1.

**Ground-based VLN Tasks.** A number of VLN tasks have been proposed for navigation on the ground. Anderson *et al.* [2] propose a Room-to-Room (R2R) navigation task, where given a detailed instruction, an agent is required to navigate from one room to another. Jain *et al.* [17] propose to concatenate existing paths in R2R to form longer paths that are not the shortest ones between starting and ending points. On the other hand, Chen *et al.* [7] propose an outdoor navigation task, TouchDown, to highlight challenges for outdoor environments. Zhu *et al.* [37] propose an object locating task, SOON, which uses detailed instruction descriptions. By contrast, Qi *et al.* [28] propose a remote object grounding task, REVERIE, with concise, high-level instructions to bet-

ter mimic the commands we humans give to each other. However, all the above-mentioned VLN tasks are designed for intelligent agents navigating on the ground, as shown in Table 1. This cannot reflect the challenges when navigating in the sky for intelligent agents like multirotor. To address this problem, in this work, we propose a new task AerialVLN, which is designed for UAV navigation in the sky.

### 3. The AerialVLN Task

As shown in Figure 1, the proposed AerialVLN task requires an intelligent agent (a multirotor in virtual environments) to fly to the destination by following a given natural language instruction and its first-person view visual perceptions provided by the simulator. Unlike previous VLN tasks [2, 20, 37], we do not provide pre-build navigation graphs in our task, so any point not occupied by objects (such as buildings and trees) is navigable. This is closer to the practical scenario.

Formally, at the beginning of each episode, the agent is placed in an initial pose  $P = [x, y, z, p, r, y']$ , where  $(x, y, z)$  denotes the agent’s position and  $(p, r, y')$  represents pitch, roll, yaw portion of the agent’s orientation. Then given a natural language instruction  $X = \langle \omega_1, \omega_2, \dots, \omega_L \rangle$ , where  $L$  is the length of instruction and  $\omega_i$  is a single word token, the agent is required to predict a series of actions. The agent can take both the instruction and visual perceptions into consideration. Although our adopted simulator can provide panoramic observations, here we follow the most robotic navigation tasks [19] setting to limit our baseline agent to the access of its front view perceptions (both depth and RGB images)  $V_t = \{v_t^R, v_t^D\}$ . The agent needs to rotate to obtain other views. Navigation ends when the agent predicts a *Stop* action or reaches a pre-defined maximum action number. The navigation is recognised as a success if the agent stops at a location that is less than 20 units to the target location, as 20 metres is the common size of a



Phenomenon	R2R[2]		ANDH[13]		TouchDown[7]		AerialVLN		Example in AerialVLN
	$p$	$\mu$	$p$	$\mu$	$p$	$\mu$	$p$	$\mu$	
Reference	100	3.7	92	1.9	100	9.2	100	<b>9.7</b>	...fly towards <b>the red bridge</b> across...
Coreference	32	0.5	8	0.1	60	1.1	68	<b>1.8</b>	...move to the next building and after reaching <b>it</b> ...
Comparison	4	0.0	32	0.4	12	0.1	20	0.2	...get to the <b>tallest</b> tree in view...
Sequencing	16	0.2	8	0.1	84	1.6	68	<b>3.7</b>	...go towards the <b>next</b> building and ...
Allocentric Relation	20	0.2	32	0.4	68	1.2	56	<b>4.6</b>	...stop <b>on</b> the middle of the bridge...
Egocentric Relation	80	1.2	32	0.4	92	3.6	100	<b>7.1</b>	... <b>stop when you get over the first tree</b> ...
Imperative	100	4.0	100	1.1	100	5.2	100	<b>6.9</b>	... <b>lift off</b> and <b>turn right</b> facing left of the old building and <b>head straight</b> ...
Direction	100	2.8	100	1.4	96	3.7	100	<b>4.6</b>	... <b>turn right and head back</b> into ...
Temporal Condition	28	0.4	20	0.2	84	1.9	76	<b>5.6</b>	...look up <b>until</b> you see the sky...
State Verification	8	0.1	20	0.2	72	1.5	28	1.3	...the road will now be <b>on your right</b> ...

Table 2: Linguistic phenomena in randomly sampled 25 instructions. AerialVLN task has a significant rate of reference, sequencing, spatial relationship and direction, which brings much more challenges to intelligent agents.  $p$  and  $\mu$  represent the percentage of instructions that present the phenomena and the average number of the phenomena appears in each instruction. For a fair comparison, TouchDown Navigation subset is used.

VLN-CE and six times TouchDown. In terms of the number of instructions, our dataset is about twice VLN-CE and RxR, four times ANDH. All these characters render our dataset extremely challenging. In Figure 3, we present the distribution of instruction length and the number of actions. As shown in Figure 3(a), instruction length ranges from 50 to 130 words. Figure 3(b) shows that most paths have 50 ~ 240 actions. These diversities make AerialVLN more challenging.

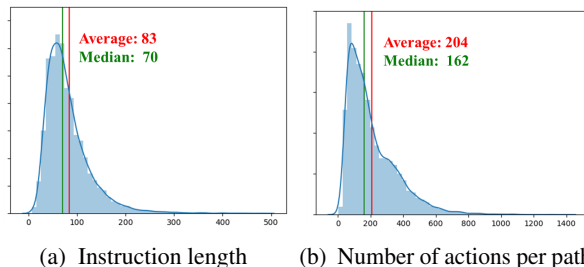


Figure 3: Instruction length and number of actions.

As in previous work [7, 20], we have also conducted statistics on linguistic phenomena of randomly sampled 25 instructions with comparison to other VLN datasets in Table 2. It shows that our AerialVLN task has a significant rate of reference, coreference, sequencing, spatial relationship and direction, which brings much more challenges.

**Dataset Split.** Following the common practice in the VLN community, we divide our dataset into the train, val\_seen, val\_unseen, and test splits. The word “seen” means the visual environments that have been seen in the train split. As shown in Table 3, we assign 17 scenes for training and val\_seen split, where the train set contains 16,380 instructions from 5,460 paths. For val\_seen, we assign 1,818 instructions from 606 paths. The val\_unseen and the test split are both assigned 8 scenes, but the test split is about double the size of the val\_unseen split, including 1610 paths with 4,830 instruc-

tions. Please note that the test split is built on unseen scenes as well and the goal locations for the test set will not be released. Instead, we provide an evaluation server where UAV trajectories can be uploaded for scoring.

Besides the standard dataset setting (with all 25 scenes), we also present a variant for small scenes, AerialVLN-S. It preserves the same split, but it has 17 scenes with a smaller scale and evenly-distributed path length, which results in a shorter path length (average path length reduces 51.5%) and shorter instruction length. In AerialVLN-S setting, the agent can sometimes even observe the goal at starting point. In this variant, there are 10, 113 instructions for the train and 333 for validation seen splits, respectively. 531 instructions are assigned for validation unseen and 771 instructions for the test set, as shown in Table 3. We hope future researchers employ AerialVLN to tackle long path length 3D VLN tasks in the unseen environment and focus on the investigation of action learning in long time horizons and sparse reward; while utilising AerialVLN-S as the benchmark for general 3D aerial VLN tasks in first-person view.

	AerialVLN			AerialVLN-S		
	Scene	Path	Instr.	Scene	Path	Instr.
Train	17	5,460	16,380	12	3,371	10,113
Val Seen	17	606	1,818	12	111	333
Val Unseen	8	770	2,310	5	177	531
Test	8	1,610	4,830	5	257	771

Table 3: Dataset splits. AerialVLN is the full dataset, and AerialVLN-S is for small scenes.

## 6. Experiment and Results

In this section, we first present the evaluation metrics and training details of baseline models. Then we provide extensive evaluation and analysis.

### 6.1. Evaluation Metrics

We adopt four widely used metrics in VLN tasks [2, 17, 20, 28]: Success Rate (SR), where one navigation is

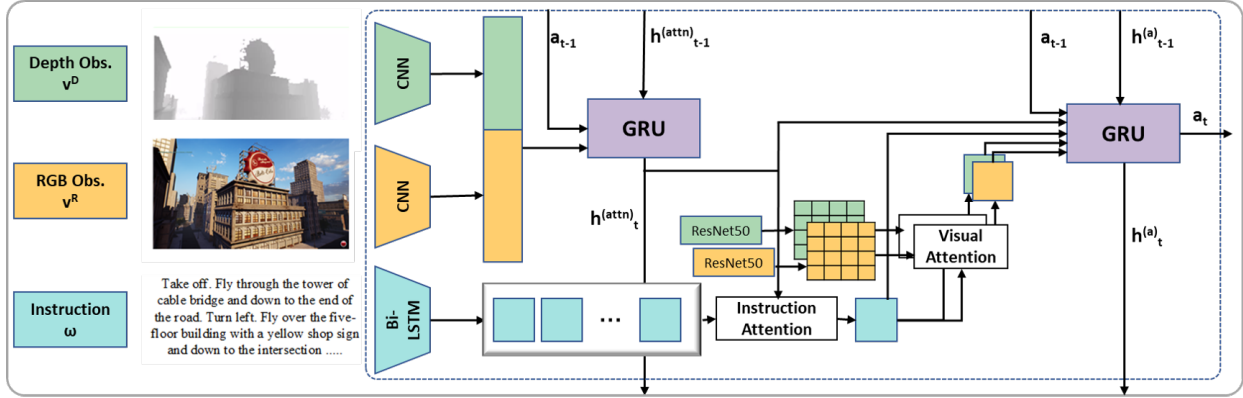


Figure 4: Main architecture of the Cross-Modal Attention model

considered successful if the agent stops within 20 meters of the destination; Oracle Success Rate (OSR), where one navigation is considered oracle success if the distance between the destination and any point on the trajectory is less than 20 meters; Navigation Error (NE), the distance between the stop location to the destination; Success rate weighted by Normalised Dynamic Time Warping (SDTW), which considers both the navigation success rate and the similarity between ground truth path and model predicted path [16].

## 6.2. Results

We evaluate five baseline models on our task. Four of these baselines have served as a golden standard for VLN tasks as in [1, 2, 28]. The other baseline is our extension to the best existing baseline. Below we first briefly introduce baselines and then present the results.

### 6.2.1 Baselines

**Random.** The agent randomly selects actions at each location and stops until the ‘stop’ action is selected or when reaching the max steps. This is widely used to reflect how big the solution space can be.

**Action Sampling.** Action Sampling agents explore the statistical characteristic of the dataset by sampling actions according to the action distribution of the training set. This can be used to measure the similarity of the action distribution on evaluation and training splits.

**LingUNet.** LingUNet [25] is a baseline model used by previously aerial VLN task LANI. Consider that LANI assume that agent can see the destination from the start point, LingUNet has an episode-wise paradigm. However, such assumption can’t stand in AerialVLN task, we thus adapt LingUNet model into a step-wise paradigm.

**Sequence-to-Sequence.** Seq2Seq [2] is a baseline model with a recurrent policy. It takes as input the concatenation of the RGB feature  $\bar{v}_t^R =$

$\text{meanpool}(\text{ResNet}_{RGB}(v_t^R))$ , the Depth feature  $\bar{v}_t^D = \text{ResNet}_{Depth}(v_t^D)$ , and the instruction embedding  $s = \text{LSTM}(\omega_1, \dots, \omega_L)$ . Then it projects them to a hidden representation  $h_t^{(a)} = \text{GRU}([\bar{v}_t^R, \bar{v}_t^D, s], h_{t-1}^{(a)})$ , which is further used to predict a distribution over the action space. The one with the largest probability is selected as the next action  $a_t = \underset{a}{\text{argmax}} \text{softmax}(W_a h_t^{(a)} + b_a)$ .

**Cross-Modal Attention.** Cross-Modal Attention (CMA) is a classical baseline model for VLN tasks. As shown in Figure 4, the CMA baseline is based on a bi-directional LSTM and divides the whole process into two parts. One is tracking visual observations, and the other one is decision-making. The former is formulated as  $h_t^{(attn)} = \text{GRU}([\bar{v}_t^R, \bar{v}_t^D, a_{t-1}], h_{t-1}^{(attn)})$ , where  $a_{t-1} \in \mathbb{R}^{1 \times 32}$  and is a learned linear embedding of the previous action. The latter encodes the instruction embedding first and outputs the intermediate hidden state  $S = \{s_1, \dots, s_L\} = \text{BiLSTM}(\omega_1, \dots, \omega_L)$ . Then the attention mechanism is applied to instructions and images, which is  $\hat{s}_t = \text{Attn}(S, h_t^{(attn)})$ ,  $\hat{v}_t^R = \text{Attn}(v_t^R, \hat{s}_t)$ ,  $\hat{v}_t^D = \text{Attn}(v_t^D, \hat{s}_t)$ , where  $\text{Attn}$  is a scaled dot-product attention. Finally, all these features and embeddings are concatenated to serve as the input of the recurrent network and predict an action for the agent to execute.

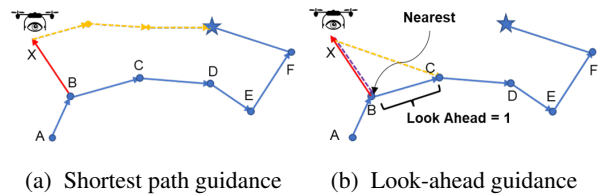


Figure 5: Illustration of Look-ahead Guidance. ‘A’ denotes starting location; ‘\*’ denotes destination; ‘X’ denotes current location; Blue path denotes ground-truth; Yellow path denotes “generated ground-truth” when the agent deviates from the real ground-truth path.

#	AerialVLN	Validation Seen				Validation Unseen				Test Unseen			
		NE/m ↓	SR/% ↑	OSR/% ↑	SDTW/% ↑	NE/m ↓	SR/% ↑	OSR/% ↑	SDTW/% ↑	NE/m ↓	SR/% ↑	OSR/% ↑	SDTW/% ↑
1	Random	300.8	0.0	0.0	0.0	351.0	0.0	0.0	0.0	356.3	0.0	0.0	0.0
2	Action Sampling	383.1	0.1	2.1	0.1	434.9	0.2	2.1	0.1	441.9	0.2	1.8	0.1
3	Seq2Seq	480.4	2.9	10.2	1.0	551.8	1.1	5.6	0.3	558.8	1.0	4.9	0.3
4	CMA	293.5	2.3	6.5	0.8	360.7	1.6	4.4	0.5	358.6	1.6	4.1	0.5
5	Human	-	-	-	-	-	-	-	-	73.5	80.8	80.8	14.2

#	AerialVLN-S	Validation Seen				Validation Unseen				Test Unseen			
		NE/m ↓	SR/% ↑	OSR/% ↑	SDTW/% ↑	NE/m ↓	SR/% ↑	OSR/% ↑	SDTW/% ↑	NE/m ↓	SR/% ↑	OSR/% ↑	SDTW/% ↑
S1	Random	109.6	0.0	0.0	0.0	149.7	0.0	0.0	0.0	148.5	0.0	0.0	0.0
S2	Action Sampling	213.8	0.9	5.7	0.3	237.6	0.2	1.1	0.1	242.0	0.7	2.5	0.3
S3	LingUNet	383.8	0.6	6.9	0.2	368.4	0.4	3.6	0.9	399.8	0.1	3.1	0.1
S4	Seq2Seq	146.0	4.8	19.8	1.6	218.9	2.3	11.7	0.7	214.6	2.2	9.4	0.7
S5	CMA	121.0	3.0	23.2	0.6	172.1	3.2	16.0	1.1	178.5	3.9	13.1	1.4
S6	Seq2Seq-DA	85.5	9.9	24.1	4.5	143.5	4.0	10.9	0.7	140.2	3.5	9.5	0.6
S7	CMA-DA	92.2	9.9	26.5	3.7	122.7	4.5	13.9	1.0	125.4	4.3	14.8	1.2
S8	Ours (LAG)	90.2	7.2	15.7	2.4	127.9	5.1	10.5	1.4	128.3	4.5	11.6	1.3

Table 4: Performance of baselines on our AerialVLN task (Row 1-5) and AerialVLN-S task (Row S1-S7). There is a significant gap to human performance.

**Look-ahead Guidance (LAG).** When training models in a student-forcing fashion, the ground-truth actions are usually determined according to the shortest path from the current location to the destination (see Figure 5(a)) in most existing methods. However, this is unreasonable because the instructions do not describe the shortest path from starting to the destination. To mitigate this issue, we inspired by [29] and propose a new strategy that generates ground-truth actions according to a “look-ahead” path. As shown in Figure 5(b), assuming the agent is at location X currently, the look-ahead path is determined by three steps: (1) find the shortest path to return to the ground-truth path ( $X \rightarrow B$  in the example); (2) navigate along the ground-truth path 10 steps (look-ahead step = 10), assuming arrive at location C; (3) the look-ahead path is the shortest path from X to location C, and the ground-truth action for the next step is the first step on this path. We combine the aforementioned CMA model and our look-ahead guidance as our new baseline, denoted as LAG.

## 6.2.2 Results

Table 4 shows all the results. The results show that:

1. Random action hardly succeeds. The success rate of the Random model (Row 1 and S1) is 0%. Even if we sample actions according to the action distribution of the training split, the success rate still remains below 1% (Row 2 and S2). Moreover, the oracle success rate is always below 3% on unseen splits. This indicates an agent can hardly reach even passing by the destination if it cannot understand the instructions, visual perceptions, and their alignment.

2. LingUNet achieves limited success. Performance on Unseen cases only slightly better than Action Sampling (Row S2~S3). This may be attributed to the lack of recurrent structures in the decision component of the

Baseline, resulting in the model’s inability to effectively model historical information.

3. The golden baselines Seq2Seq and CMA achieve success rate 1.0%~1.6% on unseen splits of the full dataset (Val\_Unseen and Test\_Unseen, Row 3~4) and 2.2%~3.9% on the AerialVLN-S dataset (Row S4~S5). At the same time, the oracle success rate also rises to 5% and 16%, respectively. This indicates that learning-based models have a larger chance to succeed than random models. However, the success rate is still rather low compared to human performance (SR: ~80%).

4. When applying the Dataset Aggregation (DA [30], an offline student-forcing strategy where executed actions are sampled from predictions instead of ground-truth actions) technique to mitigate the training-test disconnection problem (agents in test are not exposed to the consequences of their actions during training), the performance becomes better with about 6% improvement on seen split and about 1% improvement on unseen splits (Row S6~S7). This demonstrates exploring non-ground-truth actions helps learn more from training data and increases generalisation ability. On the other hand, comparing to the results of the same model (e.g., CMA-DA) on ground-based VLN tasks, such as continuous R2R, the performance on AerialVLN is rather low: SR 4.5% vs.27%. This indicates AerialVLN is much more challenging.

5. By incorporating our proposed look-ahead guidance (LAG) to the best baseline model CMA, it achieves further enhanced performance (Row S8) on unseen splits in terms of both SR and SDTW, which demonstrates the look-ahead guidance can help the agent to fly according to instructions.

We also present a qualitative result in Figure 6. It shows that when the agent can align visual and textual landmarks (as well as understand rotation commands), it

**Instruction:** *Ascend*<sup>1</sup> into the air then *turn right*<sup>2</sup> above the railway. *Turn right*<sup>3</sup> parallel with the curb. *Descend*<sup>5</sup> towards the electrical post at the intersection of the road. *Turning right*<sup>9</sup> down into the dark alleyway. *Fly to*<sup>11</sup> the end of the dark alleyway then *turning right*<sup>14</sup> at the intersection. *Stop*<sup>18</sup> near the payphones on the right side of the road.

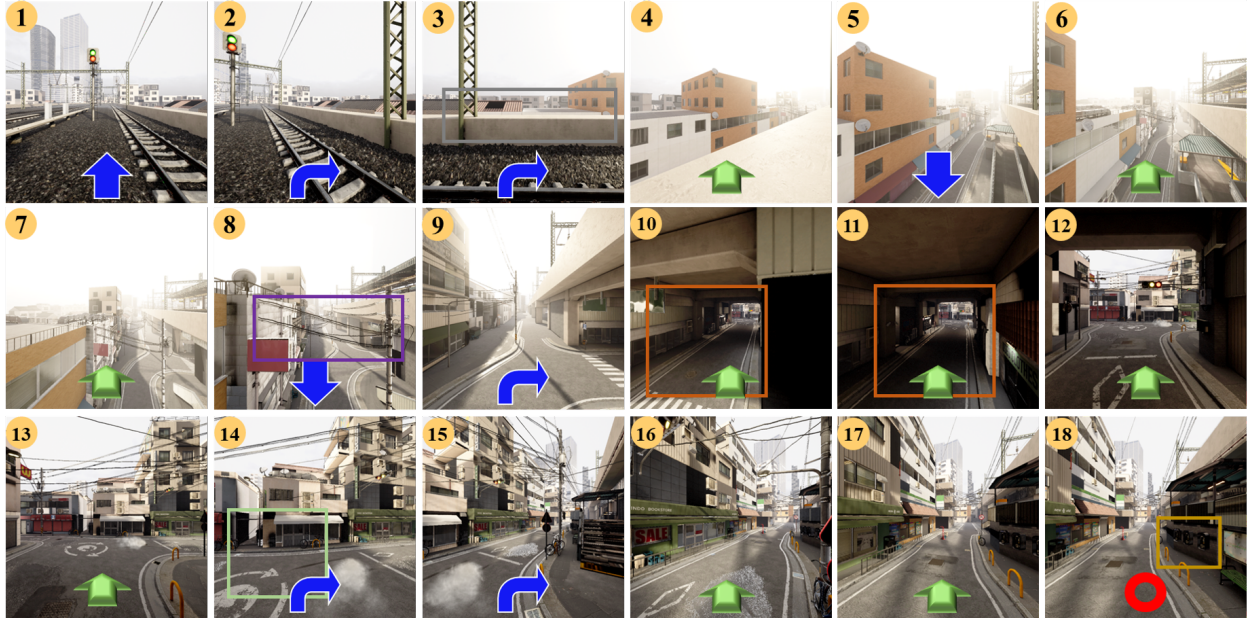


Figure 6: Visualisation of a successful navigation of our LAG model. Green arrows indicate horizontal movement motions (Move Forward, Move Left/Right); blue arrows represent vertical motion (Move Up/Down) and horizontal rotation (Turn Left/Right). The final red circle denotes Stop. We highlight aligned landmarks by coloured bounding boxes in images and words in the instruction using the same colour. The superscript of words denotes the index of the corresponding action in images.

has a large chance to succeed.

**Possible reasons for failures** We find that the length of path magnificently influences the success rate. Seq2Seq and CMA could follow instructions at an early stage but they cannot get back on track once deviate. Take AerialVLN for example, we further divide it into a long-path set (average path length 813.2m) and a short-path set (average path length 326.9m). Success rate on the former is only 1.8% while the latter can be up to 7.4%. Failure to stop correctly also leads to the low success rate. Supplementary material provides further failure analysis. As shown in Table 4, OSR of both Seq2Seq and CMA is significantly higher than SR, which suggests that the agent has passed the goal location and failed to stop around it.

### 6.3. Modality Ablation Study

To investigate the importance of different modalities in this task, we conduct an ablation study based on the CMA model via removing RGB, Depth, RGB+Depth (Vision), and Language from inputs, one by one. The results are presented in Table 5.

It shows that both the vision and language inputs play

#	Vision	Instr.	Validation Unseen			
			NE/m↓	SR/%↑	OSR/%↑	SDTW/%↑
1	RGB+D	✓	122.7	4.5	13.9	1.0
2	RGB	✓	145.5	3.2	7.9	1.0
3	D	✓	205.5	3.0	18.1	0.8
4	-	✓	177.0	1.3	12.1	0.3
5	RGB+D	-	145.4	2.1	11.1	0.5

Table 5: Modality Ablations.

the most important role (Row 1 vs. Row 4, Row 1 vs. Row 5). This is reasonable because without either of them the task actually is non-sense. Additionally, the large performance drop indicates the dataset has little visual or textual bias. On the vision side, without depth information (Row 2) or RGB information (Row 3) leads to a success rate drop and without RGB drops more. This indicates both RGB and depth information matter to the final success and RGB information contributes more.

## 7. Conclusion

In this work, we introduce a new task and a large-scale dataset, AerialVLN, for the exploration of vision-and-language navigation in the sky. The linguistic analysis yields that AerialVLN dataset presents significant challenges to complex language understanding and its associated visual-textual alignment. We also evaluate



several widely adopted baselines, of which the performance drops significantly on our task and falls far behind human performance. This indicates that our task provides a broad study space for further research.

## **8. Acknowledgement**

This work was supported by National Key R&D Program of China (No.2020AAA0106900), the National Natural Science Foundation of China (No.U19B2037), Shaanxi Provincial Key R&D Program (No.2021KWZ-03), and Natural Science Basic Research Program of Shaanxi (No.2021JCW-03).

## References

- [1] Peter Anderson, Ayush Shrivastava, Joanne Truong, Arjun Majumdar, Devi Parikh, Dhruv Batra, and Stefan Lee. Sim-to-real transfer for vision-and-language navigation. In *4th Conference on Robot Learning*, 2020.
- [2] Peter Anderson, Qi Wu, Damien Teney, Jake Bruce, Mark Johnson, Niko Sünderhauf, Ian D. Reid, Stephen Gould, and Anton van den Hengel. Vision-and-language navigation: Interpreting visually-grounded navigation instructions in real environments. In *IEEE Conference on Computer Vision and Pattern Recognition*, 2018.
- [3] Valts Blukis, Nataly Brukhim, Andrew Bennett, Ross A. Knepper, and Yoav Artzi. Following high-level navigation instructions on a simulated quadcopter with imitation learning. In *Robotics: Science and Systems XIV*, 2018.
- [4] Valts Blukis, Dipendra Kumar Misra, Ross A. Knepper, and Yoav Artzi. Mapping navigation instructions to continuous control actions with position-visitation prediction. In *2nd Annual Conference on Robot Learning, CoRL 2018, Zürich, Switzerland, 29-31 October 2018, Proceedings*, volume 87 of *Proceedings of Machine Learning Research*, pages 505–518. PMLR, 2018.
- [5] Valts Blukis, Yannick Terme, Eyvind Niklasson, Ross A. Knepper, and Yoav Artzi. Learning to map natural language instructions to physical quadcopter control using simulated flight. In Leslie Pack Kaelbling, Danica Kracic, and Komei Sugiura, editors, *3rd Annual Conference on Robot Learning, CoRL 2019, Osaka, Japan, October 30 - November 1, 2019, Proceedings*, volume 100 of *Proceedings of Machine Learning Research*, pages 1415–1438. PMLR, 2019.
- [6] Prithvijit Chattopadhyay, Judy Hoffman, Roozbeh Motlaghi, and Aniruddha Kembhavi. Robustnav: Towards benchmarking robustness in embodied navigation. In *2021 IEEE/CVF International Conference on Computer Vision, ICCV 2021, Montreal, QC, Canada, October 10-17, 2021*, pages 15671–15680. IEEE, 2021.
- [7] Howard Chen, Alane Suhr, Dipendra Misra, Noah Snaveley, and Yoav Artzi. TOUCHDOWN: natural language navigation and spatial reasoning in visual street environments. In *IEEE Conference on Computer Vision and Pattern Recognition*, 2019.
- [8] Shizhe Chen, Pierre-Louis Guhur, Makarand Tapaswi, Cordelia Schmid, and Ivan Laptev. Think global, act local: Dual-scale graph transformer for vision-and-language navigation. In *IEEE/CVF Conference on Computer Vision and Pattern Recognition, CVPR 2022, New Orleans, LA, USA, June 18-24, 2022*, pages 16516–16526. IEEE, 2022.
- [9] Jonathan Courbon, Youcef Mezouar, Nicolas Guénard, and Philippe Martinet. Vision-based navigation of unmanned aerial vehicles. *Control Engineering Practice*, 2010.
- [10] DJI. Dji drone solutions for inspection and infrastructure construction in the oil and gas industry. Website, 2022. <https://enterprise.dji.com/cn/oil-and-gas>.
- [11] DJI. Dji drone solutions for optimizing operations in the public safety industry. Website, 2022. <https://enterprise.dji.com/cn/public-safety>.
- [12] DJI. Dji drone solutions for surveying, urban planning, aec, and natural resource management. Website, 2022. <https://enterprise.dji.com/cn/surveying>.
- [13] Yue Fan, Winson X. Chen, Tongzhou Jiang, Chun ni Zhou, Yi Zhang, and Xin Wang. Aerial vision-and-dialog navigation. *ArXiv*, abs/2205.12219, 2022.
- [14] Epic Games. Unrealengine 4, 2021. <https://www.unrealengine.com/zh-CN/>.
- [15] Weituo Hao, Chunyuan Li, Xiujun Li, Lawrence Carin, and Jianfeng Gao. Towards learning a generic agent for vision-and-language navigation via pre-training. In *IEEE/CVF Conference on Computer Vision and Pattern Recognition*, 2020.
- [16] Gabriel Ilharco, Vihan Jain, Alexander Ku, Eugene Ie, and Jason Baldridge. General evaluation for instruction conditioned navigation using dynamic time warping. In *Visually Grounded Interaction and Language (ViGIL), NeurIPS 2019 Workshop*, 2019.
- [17] Vihan Jain, Gabriel Magalhães, Alexander Ku, Ashish Vaswani, Eugene Ie, and Jason Baldridge. Stay on the path: Instruction fidelity in vision-and-language navigation. In *Proceedings of the 57th Conference of the Association for Computational Linguistics*, 2019.
- [18] Liyiming Ke, Xiujun Li, Yonatan Bisk, Ari Holtzman, Zhe Gan, Jingjing Liu, Jianfeng Gao, Yejin Choi, and Siddhartha S. Srinivasa. Tactical rewind: Self-correction via backtracking in vision-and-language navigation. In *IEEE Conference on Computer Vision and Pattern Recognition*, 2019.
- [19] Jacob Krantz, Erik Wijmans, Arjun Majumdar, Dhruv Batra, and Stefan Lee. Beyond the nav-graph: Vision-and-language navigation in continuous environments. In *Computer Vision - ECCV 2020 - 16th European Conference, Glasgow, 2020*.
- [20] Alexander Ku, Peter Anderson, Roma Patel, Eugene Ie, and Jason Baldridge. Room-across-room: Multilingual vision-and-language navigation with dense spatiotemporal grounding. In *Proceedings of the 2020 Conference on Empirical Methods in Natural Language Processing*, 2020.
- [21] Alexander Ku, Peter Anderson, Roma Patel, Eugene Ie, and Jason Baldridge. Room-Across-Room: Multilingual vision-and-language navigation with dense spatiotemporal grounding. In *Conference on Empirical Methods for Natural Language Processing (EMNLP)*, 2020.
- [22] Johann Laconte, Abderrahim Kasmi, Romuald Aufrère, Maxime Vaidis, and Roland Chapuis. A survey of localization methods for autonomous vehicles in highway scenarios. *Sensors*, 2022.
- [23] Chengshu Li, Fei Xia, Roberto Martín-Martín, Michael Lingelbach, Sanjana Shrivastava, Bokui Shen, Kent Elliott Vainio, Cem Gokmen, Gokul Dharan, Tanish Jain, Andrey Kurenkov, Karen Liu, Hyowon Gweon, Jiajun Wu, Li Fei-

- Fei, and Silvio Savarese. igibson 2.0: Object-centric simulation for robot learning of everyday household tasks. In *5th Annual Conference on Robot Learning*, 2021.
- [24] Yuncheng Lu, Zhucun Xue, Gui-Song Xia, and Liangpei Zhang. A survey on vision-based UAV navigation. *Geospatial Information Science*, 2018.
- [25] Dipendra Kumar Misra, Andrew Bennett, Valts Blukis, Eyvind Niklasson, Max Shatkhin, and Yoav Artzi. Mapping instructions to actions in 3d environments with visual goal prediction. In *Proceedings of the 2018 Conference on Empirical Methods in Natural Language Processing, Brussels*, 2018.
- [26] Enrico Petritoli, Fabio Leccese, and Mariagrazia Leccisi. Inertial navigation systems for uav: Uncertainty and error measurements. In *2019 IEEE 5th International Workshop on Metrology for AeroSpace (MetroAeroSpace)*, 2019.
- [27] Yuankai Qi, Zizheng Pan, Shengping Zhang, Anton van den Hengel, and Qi Wu. Object-and-action aware model for visual language navigation. In *Computer Vision - ECCV*, 2020.
- [28] Yuankai Qi, Qi Wu, Peter Anderson, Xin Wang, William Yang Wang, Chunhua Shen, and Anton van den Hengel. REVERIE: remote embodied visual referring expression in real indoor environments. In *IEEE/CVF Conference on Computer Vision and Pattern Recognition, CVPR*, 2020.
- [29] Sonia Raychaudhuri, Saim Wani, Shivansh Patel, Unnat Jain, and Angel X. Chang. Language-aligned waypoint (LAW) supervision for vision-and-language navigation in continuous environments. In Marie-Francine Moens, Xuanjing Huang, Lucia Specia, and Scott Wen-tau Yih, editors, *Proceedings of the 2021 Conference on Empirical Methods in Natural Language Processing, EMNLP 2021, Virtual Event / Punta Cana, Dominican Republic, 7-11 November, 2021*, pages 4018–4028. Association for Computational Linguistics, 2021.
- [30] Stéphane Ross, Geoffrey J. Gordon, and Drew Bagnell. A reduction of imitation learning and structured prediction to no-regret online learning. In Geoffrey J. Gordon, David B. Dunson, and Miroslav Dudík, editors, *Proceedings of the Fourteenth International Conference on Artificial Intelligence and Statistics, AISTATS 2011, Fort Lauderdale, USA, April 11-13, 2011*, volume 15 of *JMLR Proceedings*, pages 627–635. JMLR.org, 2011.
- [31] Shital Shah, Debadepta Dey, Chris Lovett, and Ashish Kapoor. Airsim: High-fidelity visual and physical simulation for autonomous vehicles. In *Field and Service Robotics, Results of the 11th International Conference, FSR*, 2017.
- [32] Bokui Shen, Fei Xia, Chengshu Li, Roberto Martín-Martín, Linxi Fan, Guanzhi Wang, Claudia Pérez-D’Arpino, Shyamal Buch, Sanjana Srivastava, Lyne Tchapmi, Micael Tchapmi, Kent Vainio, Josiah Wong, Li Fei-Fei, and Silvio Savarese. igibson 1.0: A simulation environment for interactive tasks in large realistic scenes. In *2021 IEEE/RSJ International Conference on Intelligent Robots and Systems (IROS)*, pages 7520–7527, 2021.
- [33] Mohit Shridhar, Jesse Thomason, Daniel Gordon, Yonatan Bisk, Winson Han, Roozbeh Mottaghi, Luke Zettlemoyer, and Dieter Fox. ALFRED: A benchmark for interpreting grounded instructions for everyday tasks. In *2020 IEEE/CVF Conference on Computer Vision and Pattern Recognition, CVPR 2020, Seattle, WA, USA, June 13-19, 2020*, pages 10737–10746. Computer Vision Foundation / IEEE, 2020.
- [34] B. Sinopoli, M. Micheli, G. Donato, and T.J. Koo. Vision based navigation for an unmanned aerial vehicle. In *Proceedings 2001 ICRA. IEEE International Conference on Robotics and Automation*, 2001.
- [35] Jesse Thomason, Michael Murray, Maya Cakmak, and Luke Zettlemoyer. Vision-and-dialog navigation. In Leslie Pack Kaelbling, Danica Kragic, and Komei Sugiyama, editors, *3rd Annual Conference on Robot Learning, CoRL 2019, Osaka, Japan, October 30 - November 1, 2019, Proceedings*, volume 100 of *Proceedings of Machine Learning Research*, pages 394–406. PMLR, 2019.
- [36] Fei Xia, William B Shen, Chengshu Li, Priya Kasimbeg, Micael Edmond Tchapmi, Alexander Toshev, Roberto Martín-Martín, and Silvio Savarese. Interactive gibbon benchmark: A benchmark for interactive navigation in cluttered environments. *IEEE Robotics and Automation Letters*, 5(2):713–720, 2020.
- [37] Fengda Zhu, Xiwen Liang, Yi Zhu, Qizhi Yu, Xiaojun Chang, and Xiaodan Liang. SOON: scenario oriented object navigation with graph-based exploration. In *IEEE Conference on Computer Vision and Pattern Recognition, CVPR*, 2021.